

**INVESTIGATION OF TRACTION PATTERNS AND
FORCES OF SINGLE QUIESCENT AND
MIGRATORY KERATINOCYTES USING A NOVEL
CELL TRACTION FORCE MICROSCOPY
TECHNIQUE**

DR. SOON CHIN FHONG

DR. MORGAN DENYER

ASSOCIATE PROF. DR. NAFARIZAL NAYAN

PROF. DR. HASHIM BIN SAIM

GERAN FRGS

NO. VOT : FRGS 1050

UNIVERSITI TUN HUSSEIN ONN MALAYSIA

ABSTRACT

Keratinocyte traction forces play a crucial role in wound healing. The aim of this study was to develop a novel cell traction force (CTF) transducer system based on cholesteryl ester liquid crystals (LC). The CTF microscopy system is used to analyse the traction force patterns of quiescent and migratory keratinocytes cultured on LC. We report the application of the WSPR imaging system in the study of the interaction between keratinocytes and liquid crystals (LC). Imaging of fixed keratinocytes cultured on gold coated surface plasmon substrates functionalized with a thin film of liquid crystals was performed in air using a 1.45 NA objective based system. Characteristics of the cell integrin expressions and presence of extracellular matrix (ECM) proteins on the liquid crystals were interrogated using various immunocytochemical techniques, Atomic Force Microscopy (AFM), fourier transform infrared spectroscopy (FTIR). The generated CTF map highlighted distinct distributions and different magnitude of CTFs were revealed for polarized and non-polarized keratinocytes. WSPR imaging indicated that keratinocytes are less spread and formed distinct topography of cell-liquid crystal couplings when cultured on liquid crystal coated substrates. The WSPR microscopy reveals that the cells remodeled their topography of adhesion at different interfaces. The immunostainings indicated that cell adhesion on the LC is mediated by self-secreted ECM proteins. As revealed by the AFM imaging, the constraint in cell membrane spread on the LC leads to the increase in cell surface roughness and thickness of cell membrane. The biophysical expressions of cells on biocompatible CELC suggested that CELC could be a new class of biological relevant material.

TABLE OF CONTENTS

LIST OF PUBLICATION.....	ii
ACKNOWLEDGEMENT	iii
STATEMENT OF ORIGINALITY.....	iv
ABSTRACT.....	v
TABLE OF CONTENTS.....	vii
TABLE OF FIGURES.....	viii
LIST OF FIGURES.....	x
1 INTRODUCTION	1
1.1 Introduction.....	1
1.2 Research Background	5
1.3 Aim and Objectives of the Research.....	8
2 DEVELOPMENT OF A NOVEL LIQUID CRYSTAL BASED CELL TRACTION FORCE TRANSDUCER.....	9
2.1 Introduction.....	9
2.2 Materials and Methods.....	11
2.2.1 Preparation of liquid crystal substrates.....	11
2.2.2 Spherical indentation	11
2.2.3 Cell culture	11
2.2.4 Staining for actin fibers and vinculin accumulations	12
2.2.5 Cell relaxation experiment and quantification of cell traction forces.....	12
2.2.6 Development of a Cell Traction Force Measurement and Mapping Software	15

2.3	Results and Discussion.....	16
3	INTERFACIAL STUDY OF CELL ADHESION TO LIQUID CRYSTALS USING WIDEFIELD SURFACE PLASMON RESONANCE MICROSCOPY	24
3.1	Introduction.....	24
3.2	Materials and Methods.....	26
3.2.1	Simulation of widefield surface plasmon resonance profiles	26
3.2.2	Cell culture and preparation of imaging sample	29
3.2.3	Widefield surface plasmon resonance imaging of cell-liquid crystal interface	30
3.2.4	Immunocytochemical Staining of Vinculin and Nucleus	31
3.2.5	Statistical analysis.....	31
3.3	Results and discussion.....	32
4	BIOPHYSICAL CHARACTERISTICS OF CELLS CULTURED ON CHOLESTERYL ESTER LIQUID CRYSTALS	40
4.1	Introduction.....	40
4.2	Materials and methods.....	41
4.2.1	Cell culture	41
4.2.2	Preparation of liquid crystal substrates.....	41
4.2.3	Immunofluorescence staining of integrins.....	42
4.2.4	Laminin staining.....	43
4.2.5	Immunoperoxidase staining of collagen type IV.....	44
4.2.6	Immunofluorescence staining of fibronectin	44
4.2.7	Preparation of liquid crystal substrate for polarizing microscopy....	45
4.2.8	Liquid crystal sample preparation and FTIR	45
4.2.9	Characterizing cell surface with atomic force microscopy.....	46
4.3	Results and discussion.....	46

5	TRACKING TRACTION FORCE CHANGES SINGLE CELLS ON THE LIQUID CRYSTAL SURFACE	54
5.1	Introduction.....	54
5.2	Experimental section.....	56
5.2.1	Preparation of liquid crystal substrate	56
5.2.2	Preparation of human keratinocyte cell lines.....	56
5.2.3	Culturing cells on the liquid crystal substrates.....	56
5.2.4	Staining for actin fibers and vinculin accumulations.....	57
5.2.5	Quantification of cell traction forces using cell traction force mapping software.....	57
5.3	Results and discussion.....	58
5.4	Conclusions.....	65
6	CONCLUSION	66
	REFERENCE	68
	APPENDIX A: Spherical Indentation and Cell Traction Force Measurement Software Development Technique.....	76
	APPENDIX B: The Associated Publication.....	84

LIST OF FIGURES

Figure 2-1. (a) Schematic diagrams showing lateral view of a cell inducing deformations in the liquid crystal surface due to the contractions of circumferential actin filaments exerting traction forces via focal adhesions. (b) A constitutive model showing the dimensions of a stress site in LC surface before (solid line) and after (broken line) the compressive force (F) applied to the stress plane (A). (x, y) and (x_o, y_o) are the dimensions of biaxial deformation during relaxation and contraction, respectively. The parameters, x and y , are the dimensions in transverse and longitudinal directions, respectively. 14

Figure 2-2. Fluorescence micrographs of staining against (a) actin filaments, and (b) vinculin for keratinocytes cultured on the liquid crystal substrates. (Scale bar: 25 μm)..... 16

Figure 2-3. Phase contrast images of a cell treated with 30 μM cytochalasin-B at (a) 0 minute, (b) 30 minute and (c) 60 minutes on the surface of the liquid crystals, (Scale bar: 20 μm); (d) Enlarged exert of a box in (a) showing the width of the deformation lines formed in the LC surface, (Scale bar: 10 μm). The inward and outward arrows show the directions of the applied and released forces at a stress site, respectively. (e) Transverse displacement (Δx) versus the length of longitudinal deformation (y_o), (f) cell traction force (F) versus the transverse displacement (Δx), and (g) cell traction force (F) versus the length of longitudinal deformation (y_o) for 55 deformation lines. 18

Figure 2-4. (a) Distribution of cell traction force points on a Euclidean coordinate system and (b) the associated 3D force map rendered in pseudo-colors. Phase contrast photomicrographs of (c) a single quiescent and (d) a polarized HaCaTs contracting on the LC based CTF transducer. Images on the right of (c) and (d) are the associated force maps for the cells in (c) and (d), respectively. The scale bar in pseudo colors represents the intensity of the cell traction forces in nano-Newton. (Scale bar: 20 μm)..... 21

CHAPTER 1

INTRODUCTION

1.1 Introduction

Pharmacology is an experimental science which involves studying the effects of chemically active molecules on physiological activity. As one of the cornerstones in new drug development, pharmacology investigates the effects of new drugs through screening for desired activity, determining the mode of actions and defining the drug therapeutic function. *Pharmacological studies involving animals in biological assays started as early as the 19th century (Fastier and Reid, 1949). Mammals such as rats, guinea pigs, rabbits and dogs are the most commonly used experimental subjects. In pre-clinical testing, organs or tissues are excised surgically and prepared for pharmacological study in oxygenated physiological solution within an organ bath. The organ bath technique was first applied by Henrick Magnus in 1904 on a strip of small intestine (Fastier and Reid, 1949). Today, the organ bath is still being used extensively to investigate the physiology and pharmacology of various tissues such as muscle, arterial rings, uterine tissue, ileum, colon arterial and diaphragm. In an organ bath, a section of tissue is suspended between a fixed point and an isotonic or isometric force transducer in a pre-warmed Krebs solution (Bennett and Pettigrew, 1974). Rhythmic contraction and relaxation of the tissue creates variable load forces which the force transducer converts into electrical signals (Bennett and Pettigrew, 1974). In modern systems, the electrical signals are digitised and displayed on a computer monitor as traces of contractility. Stimulation of the tissue can be induced by chemical, electrical or physical means. The range of*

sensitivity in terms of force transduction of commercial systems is from 50 μN to 250 mN (ADINSTRUMENT Incorporation and DMT Incorporation).

New developments in the agricultural and pharmaceutical industries require stringent evaluation and assessment of compounds before clinical trials. Prudent pre-clinical trials usually involve large numbers of rodent and non-rodent mammalian species (Ganter et al., 2005, Jacobson-Kram and Mills, 2008). Recently, the United States Food and Drug Administration (FDA) issued a guide on Exploratory Investigational New Drug (IND) to reduce animal exploitation and simultaneously to accelerate the development of new pharmaceutical agents (Jacobson-Kram and Mills, 2008). Similarly, a new directive concerning cosmetic products (2000/0077(COD)) aims at reducing animal testing by promoting the design of in-vitro toxicological assays. Thus, cell line based culture assays are attracting interest as an alternative for drug and cosmetic testing. However, to enable this highly sensitive and high throughput screening, accurate analytical techniques for sensing cellular activities are required. During pre-clinical testing, application of an agonist and an antagonist to a tissue in an organ bath induces contraction and relaxation of a tissue, which is measured in terms of force. The question is how did the drug trigger the action of the tissue? This analysis in a tissue constructed from many different cells types is difficult (for example, the same section of tissue may contain neurons, smooth muscle cells and fibroblasts), thus, the characterisation of cell physiological responses may provide more insights if determined by examining the contractile properties of the individual cells (Bitar and Makhlof, 1985, Li et al., 2009, Ma et al., 2002).

Motivated by the need to assess single cell contraction induced by chemical stimuli, contractility assays measuring the change in average cell length of a large population of smooth muscle cells were developed to study the responses of smooth muscle to agonists such as endothelin-1, interleukin, C-terminal octapeptide of cholecystokinin, acetylcholine and methoionine-enkephalin (Bitar and Makhlof, 1985, Moumami and Woodford, 1992, Dallot et al., 2003, Akiho et al., 2002). These studies identified a number of advantages of single cell based biological assays for the pharmaceutical industry such as: (a) the easy characterisation of surface receptors as a consequent of drug action, and (b) highly repeatable screening (Dallot et al., 2003, Akiho et al., 2002).

Thereafter, many single cell based biosensors have been developed for use in pharmacological screening (Stenger et al., 2001, Park and Shuler, 2003). In a cell based biosensor system, the cell is the primary detector which converts the molecular signals into electrophysiological or mechanical signals; these signals are then transduced by a secondary transducer in the form of electrode, magnetic or optical detector. Overall, the techniques in measuring physiological responses of single living cells to analytes can be classified into two broad categories: electrophysiology and mechanobiological measurement systems. Each category has its own advantages and disadvantages.

Electrophysiological techniques originated from neuroscience, in which, systems were developed to study the electrical activity of nerves cells (Hodgkin and Keynes, 1955, Hodgkin, 1937, Gross et al., 1972). These systems have since been employed to study other electrogenic cells such as smooth muscle and cardiac myocytes (Thomas, 1972, Hara et al., 1986, Cranefield and Hoffman, 1958). These techniques involve the use of electrodes to sense the depolarisation or hyperpolarisation of action potential of cells attaching to the electrodes (Gross et al., 1972). Patch clamp (Kraft and Patt, 2006, Betz. W. J. and Sakmann, 1971), potassium chloride filled glass electrode (Dole, 1941) and planar patch clamp (Behrends and Fertig, 2007) technique are among the classical electrophysiology techniques developed to monitor the activities of individual ionic channels in the cell membrane. In these systems, the recording can be intracellular or extracellular in a cell culture. Unfortunately, these techniques are time consuming and because of their invasive nature, they often result in cell death. One of the alternatives is monitoring cell electrophysiology using micro-fabricated extracellular electrode recording or microelectrode array systems (Kovacs, 2003, Fromherz, 2003). These systems rely on culturing electrogenic cells over miniaturised recording sites made of gold or indium-tin-oxide, or arrays of field effect transistor electrodes to monitor signals from those cells directly position over the recording sites (Fromherz, 2003, Kovacs, 2003, Thomas et al., 1972, Gross et al., 1977, Offenhausser et al., 1997). These systems have been used to generate dose response curves for known pharmacological agents (Yu et al., 2006) but are subject to limitations associated with sensitivity and reliability (Muthuswamy et al., 2005, Shoham et al., 2006)

In the measurement systems using microelectrode, the electrodes allow recording of electrical activity at single point of the cell membrane or tissue but this does not

provide information about the spatial distribution of bioelectric activity over the cell membrane (Loew, 1996). To circumvent this issue, an optical electrophysiology technique has been developed which involves the use of potential-sensitive dyes or fluorescing proteins that are capable of changing the fluorescence intensity when these probes detected sub-millisecond membrane potential changes or intrinsic birefringence (Obaid et al., 2004, Cohen and Salzeberg, 1978, Loew, 1996). The potential-dependent characteristic is able to shift the excitation spectra, and thus allowing the quantification of membrane potential (Waggoner, 1979, Cohen and Salzeberg, 1978). After the tissue or cell is perfused or injected with the potential sensitive dye, two-dimensional (2D) distribution of colour intensity along the cell membrane corresponding to the field potential can be visualised and recorded. Some dyes developed earlier such as cyanine dyes are believed to inhibit the metabolic activity or inducing photodynamic damage due to the strong illumination of these dyes (Waggoner, 1979, Obaid et al., 2004). Therefore, the potentiometric dyes developed later (Potential-sensitive ANEP dyes, Invitrogen) aim to overcome these problems. These dyes improved the signal to noise ratio and reducing dye internalisation (absorption into the nucleus). However, these dyes still needed to be solubilised in dimethyl sulfoxide (DMSO) and are limited by moderate phototoxicity (Obaid et al., 2004). Phototoxicity increases oxygen radicals in cell cultures and can be cytotoxic in the long term (Obaid et al., 2004). Electrophysiological measurements are more suitable for electrogenic cells that fire large action potentials. Monitoring the physiological changes of epithelial cells is more related to the measurement of cell mechanical activity in terms of forces (for example, contraction or traction forces). Traction forces are defined as forces that a cell exerts tangentially on a substrate (Oliver et al., 1998). They are the indications of the contractile forces generated within the cell cytoskeletons. Studies on how the contraction forces are generated and transmitted by a single cell as traction forces to the adjacent cell and extracellular matrix (ECM) set the foundation for the development of cell traction force (CTF) measurement technique.

1.2 Research Background

Pharmacology is an experimental science which involves studying the effects of chemically active molecules on physiological activity. As one of the cornerstones in new drug development, pharmacology investigates the effects of new drugs through screening for desired activity, determining the mode of actions and defining the drug therapeutic function. Pharmacological studies involving animals in biological assays started as early as the 19th century (Fastier and Reid, 1949). Mammals such as rats, guinea pigs, rabbits and dogs are the most commonly used experimental subjects. In pre-clinical testing, organs or tissues are excised surgically and prepared for pharmacological study in oxygenated physiological solution within an organ bath. The organ bath technique was first applied by Henrick Magnus in 1904 on a strip of small intestine (Fastier and Reid, 1949). Today, the organ bath is still being used extensively to investigate the physiology and pharmacology of various tissues such as muscle, arterial rings, uterine tissue, ileum, colon arterial and diaphragm. In an organ bath, a section of tissue is suspended between a fixed point and an isotonic or isometric force transducer in a pre-warmed Krebs solution (Bennett and Pettigrew, 1974). Rhythmic contraction and relaxation of the tissue creates variable load forces which the force transducer converts into electrical signals (Bennett and Pettigrew, 1974). In modern systems, the electrical signals are digitised and displayed on a computer monitor as traces of contractility. Stimulation of the tissue can be induced by chemical, electrical or physical means. The range of sensitivity in terms of force transduction of commercial systems is from 50 μ N to 250 mN (ADINSTRUMENT Incorporation and DMT Incorporation).

New developments in the agricultural and pharmaceutical industries require stringent evaluation and assessment of compounds before clinical trials. Prudent pre-clinical trials usually involve large numbers of rodent and non-rodent mammalian species (Ganter et al., 2005, Jacobson-Kram and Mills, 2008). Recently, the United States Food and Drug Administration (FDA) issued a guide on Exploratory Investigational New Drug (IND) to reduce animal exploitation and simultaneously to accelerate the development of new pharmaceutical agents (Jacobson-Kram and Mills, 2008). Similarly, a new directive concerning cosmetic products (2000/0077(COD)) aims at reducing animal testing by promoting the design of in-vitro toxicological assays. Thus, cell line based culture assays are attracting interest

as an alternative for drug and cosmetic testing. However, to enable this highly sensitive and high throughput screening, accurate analytical techniques for sensing cellular activities are required. During pre-clinical testing, application of an agonist and an antagonist to a tissue in an organ bath induces contraction and relaxation of a tissue, which is measured in terms of force. The question is how did the drug trigger the action of the tissue? This analysis in a tissue constructed from many different cells types is difficult (for example, the same section of tissue may contain neurons, smooth muscle cells and fibroblasts), thus, the characterisation of cell physiological responses may provide more insights if determined by examining the contractile properties of the individual cells (Bitar and Makhlof, 1985, Li et al., 2009, Ma et al., 2002).

Motivated by the need to assess single cell contraction induced by chemical stimuli, contractility assays measuring the change in average cell length of a large population of smooth muscle cells were developed to study the responses of smooth muscle to agonists such as endothelin-1, interleukin, C-terminal octapeptide of cholecystokinin, acetylcholine and methoionine-enkephalin (Bitar and Makhlof, 1985, Moumami and Woodford, 1992, Dallot et al., 2003, Akiho et al., 2002). These studies identified a number of advantages of single cell based biological assays for the pharmaceutical industry such as: (a) the easy characterisation of surface receptors as a consequent of drug action, and (b) highly repeatable screening (Dallot et al., 2003, Akiho et al., 2002).

Thereafter, many single cell based biosensors have been developed for use in pharmacological screening (Stenger et al., 2001, Park and Shuler, 2003). In a cell based biosensor system, the cell is the primary detector which converts the molecular signals into electrophysiological or mechanical signals; these signals are then transduced by a secondary transducer in the form of electrode, magnetic or optical detector. Overall, the techniques in measuring physiological responses of single living cells to analytes can be classified into two broad categories: electrophysiology and mechanobiological measurement systems. Each category has its own advantages and disadvantages.

Electrophysiological techniques originated from neuroscience, in which, systems were developed to study the electrical activity of nerves cells (Hodgkin and Keynes, 1955, Hodgkin, 1937, Gross et al., 1972). These systems have since been employed to study other electrogenic cells such as smooth muscle and cardiac

myocytes (Thomas, 1972, Hara et al., 1986, Cranefield and Hoffman, 1958). These techniques involve the use of electrodes to sense the depolarisation or hyperpolarisation of action potential of cells attaching to the electrodes (Gross et al., 1972). Patch clamp (Kraft and Patt, 2006, Betz. W. J. and Sakmann, 1971), potassium chloride filled glass electrode (Dole, 1941) and planar patch clamp (Behrends and Fertig, 2007) technique are among the classical electrophysiology techniques developed to monitor the activities of individual ionic channels in the cell membrane. In these systems, the recording can be intracellular or extracellular in a cell culture. Unfortunately, these techniques are time consuming and because of their invasive nature, they often result in cell death. One of the alternatives is monitoring cell electrophysiology using micro-fabricated extracellular electrode recording or microelectrode array systems (Kovacs, 2003, Fromherz, 2003). These systems rely on culturing electrogenic cells over miniaturised recording sites made of gold or indium-tin-oxide, or arrays of field effect transistor electrodes to monitor signals from those cells directly positioned over the recording sites (Fromherz, 2003, Kovacs, 2003, Thomas et al., 1972, Gross et al., 1977, Offenhausser et al., 1997). These systems have been used to generate dose response curves for known pharmacological agents (Yu et al., 2006) but are subject to limitations associated with sensitivity and reliability (Muthuswamy et al., 2005, Shoham et al., 2006)

In the measurement systems using microelectrode, the electrodes allow recording of electrical activity at single point of the cell membrane or tissue but this does not provide information about the spatial distribution of bioelectric activity over the cell membrane (Loew, 1996). To circumvent this issue, an optical electrophysiology technique has been developed which involves the use of potential-sensitive dyes or fluorescing proteins that are capable of changing the fluorescence intensity when these probes detected sub-millisecond membrane potential changes or intrinsic birefringence (Obaid et al., 2004, Cohen and Salzeberg, 1978, Loew, 1996). The potential-dependent characteristic is able to shift the excitation spectra, and thus allowing the quantification of membrane potential (Waggoner, 1979, Cohen and Salzeberg, 1978). After the tissue or cell is perfused or injected with the potential sensitive dye, two-dimensional (2D) distribution of colour intensity along the cell membrane corresponding to the field potential can be visualised and recorded. Some dyes developed earlier such as cyanine dyes are believed to inhibit the metabolic activity or inducing photodynamic damage due to the strong

illumination of these dyes (Waggoner, 1979, Obaid et al., 2004). Therefore, the potentiometric dyes developed later (Potential-sensitive ANEP dyes, Invitrogen) aim to overcome these problems. These dyes improved the signal to noise ratio and reducing dye internalisation (absorption into the nucleus). However, these dyes still needed to be solubilised in dimethyl sulfoxide (DMSO) and are limited by moderate phototoxicity (Obaid et al., 2004). Phototoxicity increases oxygen radicals in cell cultures and can be cytotoxic in the long term (Obaid et al., 2004).

Electrophysiological measurements are more suitable for electrogenic cells that fire large action potentials. Monitoring the physiological changes of epithelial cells is more related to the measurement of cell mechanical activity in terms of forces (for example, contraction or traction forces). Traction forces are defined as forces that a cell exerts tangentially on a substrate (Oliver et al., 1998). They are the indications of the contractile forces generated within the cell cytoskeletons. Studies on how the contraction forces are generated and transmitted by a single cell as traction forces to the adjacent cell and extracellular matrix (ECM) set the foundation for the development of cell traction force (CTF) measurement technique.

1.3 Aim and Objectives of the Research

The primary aim of this research is to develop a novel liquid crystal based cell traction force transducer (LCTFT) system that can be used to determine the effects of pharmacological agents on the forces exerted by single cells on a liquid crystal substrate. In order to achieve this aim, this thesis will:-

- 1) To develop a technique in quantifying the cell traction force exerted on the liquid crystal substrate.
- 2) To study the morphology of single quiescent and migratory keratinocytes attaching to the liquid crystal based cell force transducer.
- 3) To measure and map the traction force patterns of single quiescent and migratory keratinocytes in a 3D force distribution map.

CHAPTER 2

DEVELOPMENT OF A NOVEL LIQUID CRYSTAL BASED CELL TRACTION FORCE TRANSDUCER

2.1 Introduction

A cell traction force (CTF) is defined as a tangential tension exerted by cells to the underlying substrate [1]. Cell tractions are associated with the contractility of the actin cytoskeleton which regulate important physiological processes such as cytokinesis, cell morphogenesis and cell migration [2-4]. Cell generated tension can be measured using various CTF sensing techniques. The most promising techniques are the soft substrate stretching techniques because these techniques measure single cell traction forces by direct observation via microscopy without the need for sophisticated instruments [5]. The soft substrate stretching technique often involves the use of polymers such as silicone rubber, polyacrylamide (PAA), polydimethylsiloxane (PDMS) and collagen gel, for which, the measurements of the cell traction forces (CTFs) are based on the strain of surfaces induced by cell tractions [4, 6-8]. The strain measured from the soft substrate material is either in the form of wrinkles or displacements of fluorescence markers. However, these polymer stretching techniques are limited by spatial resolution or the lack of ability to detect localized CTFs mainly due to the nonlinear viscoelastic behavior of the polymers at low shear rates [5, 9-11]. With highly cross-linked molecules in the polymers, the intracellular energy transferred from the cells to the surfaces tends to propagate to neighboring regions, leading to the formation of uncorrelated and chaotic deformations in the surfaces [5, 12]. Due to the nonlinear behavior of the wrinkles formed, no suitable computational solution has been identified for solving the

complex problems of surface wrinkles generated by a single cell [13]. Polymer based micro-cantilever or micro-patterning techniques demonstrated the ability to probe isolated traction forces exerted by cells. However, these techniques that were previously applied in cell contact guidance have a large influence on cell behavior and a limit in detectable CTFs [5, 14-17].

Semi-solid liquid crystals (LCs) characterized by highly compacted arrangements of molecules do provide an alternative for probing the traction forces of cells with high flexibility and sensitivity. In the context of biocompatibility, Shear sensitive cholesteryl ester liquid crystals (CELC) have been shown to be non-toxic, provide affinity for cell attachment and are thermally stable between 20 °C and 50 °C [18]. Rheological characterizations of this material show that CELC after incubated in the cell culture media at 37 °C for 48 hours exhibits a linear viscoelastic behaviour under low rates of shear ($< 1 \text{ s}^{-1}$) and within 10% of shear strain [19]. This indicates that CELC exhibit a linear viscoelastic behaviour in response to external shear stress and are very sensitive to physical restructuring of cells as demonstrated previously [20]. Nonetheless, the cholesteryl ester liquid crystals consist of compounds which were derived from cholesterol [21]. Cholesterol moieties have been shown to enhance the physical properties of cells during attachment and proliferations [22].

Driven by the potential of liquid crystals to circumvent the problems presented by polymer based CTF sensors, the aim of this study was to develop a force transducer based on CELC which can transduce the traction forces of single human keratinocytes into linearly quantifiable mechanical deformations. Traction forces produced by the keratinocytes are central to the study of wound repair [23-25]. Measuring these traction forces will have relevance for research into skin grafts as the impact of cell contraction on shrinkage of skin constructs prior to grafting is significant [26, 27]. In order to quantify the CTF using linear elastic theory, the Young's modulus and strain of the CELC needed to be determined. In this paper, the spherical indentation technique will be used to determine the Young's modulus of the CELC. A new microscopy technique for profiling the biaxial strain of deformation lines induced by the CTFs of cells on the LC surfaces will be described. This technique involves relaxation of cells with an actin depolymerisation solution (cytochalasin-B) which leads to the release of CTFs. Hence, the displacements in transverse and longitudinal directions for a deformation line can be derived and

estimated. Based on Hooke's equation and small deformation theories, the linear CTF-deformation relationships for the LCs in a biaxial direction were approximated. In order to map the forces underlying single cells, the development of a custom-built cell traction force mapping (CTFM) software will be described.

2.2 Materials and Methods

2.2.1 Preparation of liquid crystal substrates

Ester based cholesteryl liquid crystal [28] gel and coating of the liquid crystal (LC) substrates were as reported in [19]. Three LC substrates at a thickness (t) of ~ 100 μm were prepared and each placed in a petri dish containing Roswell Park Memorial Institute-1640 (RPMI-1640, Sigma Aldrich, UK) culture media and incubated at 37 $^{\circ}\text{C}$ for 24 hours. After incubation, the LC substrates were ready for spherical indentation.

2.2.2 Spherical indentation

Spherical indentation has become a common method to determine the Young's modulus of soft gels because this technique provides small strain deformation in biaxial directions and making it applicable to permeable or semi permeable membranes [29, 30]. In this experiment, the Young's modulus of the LC substrates in cell culture media was determined by using an extended model derived from the theory of Hertz's contact mechanics [30]. This involved the consideration of the finite thickness of the sample. The detail description of the spherical indentation technique is as described in the Appendix A.

2.2.3 Cell culture

A human keratinocyte cell line (HaCaT) was generously purchased from Cell Line Services (CLS, Germany). The cells in the culture flasks were maintained in RPMI-1640 media supplemented with fetal calf serum (PromoCell, UK), L-glutamine (2 mM, Sigma Aldrich, UK), fungizone (2.5 mg/l, Sigma Aldrich, UK), penicillin (100 units/ml, Sigma Aldrich, UK) and streptomycin (100 mg/ml, Sigma Aldrich, UK).

These cells were harvested using standard cell culture procedures and seeded onto two LC substrates in separate petri dishes, each at a density of 1.3×10^3 cells/cm².

2.2.4 Staining for actin fibers and vinculin accumulations

After the HaCaT cells were cultured on the LC substrates and incubated at 37 °C for 24 hours, one of the LC substrates was removed from the petri dish and washed twice with Hanks Balanced Salt Solution (HBSS, Sigma Aldrich, UK). Subsequently, the cells were fixed with 1% formaldehyde in HBSS for 6 minutes, rinsed twice with HBSS and permeabilized with 0.1% Triton X-100 for 3 minutes. To stain the F-actin after washing, the cells were incubated for 45 minutes with 1 µg/ml of Fluorescence isothiocyanate (FITC) labeled Phalloidin solution (Sigma Aldrich, UK) in HBSS followed by another three washes in HBSS. To stain the nuclei, 0.1 µg/ml of DAPI dihydrochloride solution (Sigma Aldrich, UK) in HBSS was applied to the cells for 15 minutes before microscopy.

HaCaT cells cultured on another LC substrate were immuno-stained for vinculin expressions using procedures as reported in [31]. All the fluorescence stained samples were observed using a plan fluor oil immersion lens of a Nikon Eclipse 80i fluorescence microscope (N.A of 1.3, 100x magnification) under dark field (DF) illumination and the images were captured using a digital camera linked to the ACT-2u software. The resolution of this fluorescence microscope is 0.23 µm. Blue (nuclei) and green (actin and vinculin) staining images were digitally merged using ImageJ software. All fluorescence staining experiments for actin and vinculin were repeated three times. The width of the vinculin staining was measured in ImageJ and expressed as means ± standard error (SE).

2.2.5 Cell relaxation experiment and quantification of cell traction forces

HaCaT cells at a cell density of 500 cells/cm² were plated onto a petri dish containing a LC substrate and incubated at 37 °C for 24 hours. In this experiment, extracellular matrix proteins were not applied to the LC substrates. The omission of surface treatment with adhesion proteins is based on the assumption that keratinocytes are capable of secreting their own basement membrane in the in-vitro cultures [32, 33]. After incubation, the cultured cells were found to adhere and

contract on the LC surfaces while inducing deformation lines as a result of localized compression in transverse directions at the margin of a cell as shown in Figure 2-1. The transverse displacement (Δx) of the cell induced deformation lines due to the contractions of the actin filaments was determined by treatment with an actin depolymerization solution, cytochalasin-B [34]. The adherent cells on the LC surface were treated with 5 μ l of 30 μ M cytochalasin-B at 37 $^{\circ}$ C for one hour. Cytochalasin-B (35 mg/ml, Sigma Aldrich, UK) was solubilised in 0.042% (v/v) ethanol (in distilled water). The use of 30 μ M of cytochalasin B for cell relaxation is well established as reported in [34-36]. During treatments, the petri dish containing the cells cultured on the LC substrate was placed on a heating stage maintained at 37 $^{\circ}$ C while time lapse images were captured every five minutes for an hour via a GX-XDS2 phase contrast microscope equipped with a GT VisionCX digital camera. In the phase contrast microscope used, a long distance flat field achromatic objective lens (40x magnification) with a numerical aperture (NA) of 0.65 was used under an illumination of halogen incandescent light source housed in a dichroic reflector ($\lambda = 400 - 700$ nm). The resolution of this phase contrast microscope is 0.38 μ m. The cell relaxation experiment was repeated for a randomly selected cell from ten similar cultures.

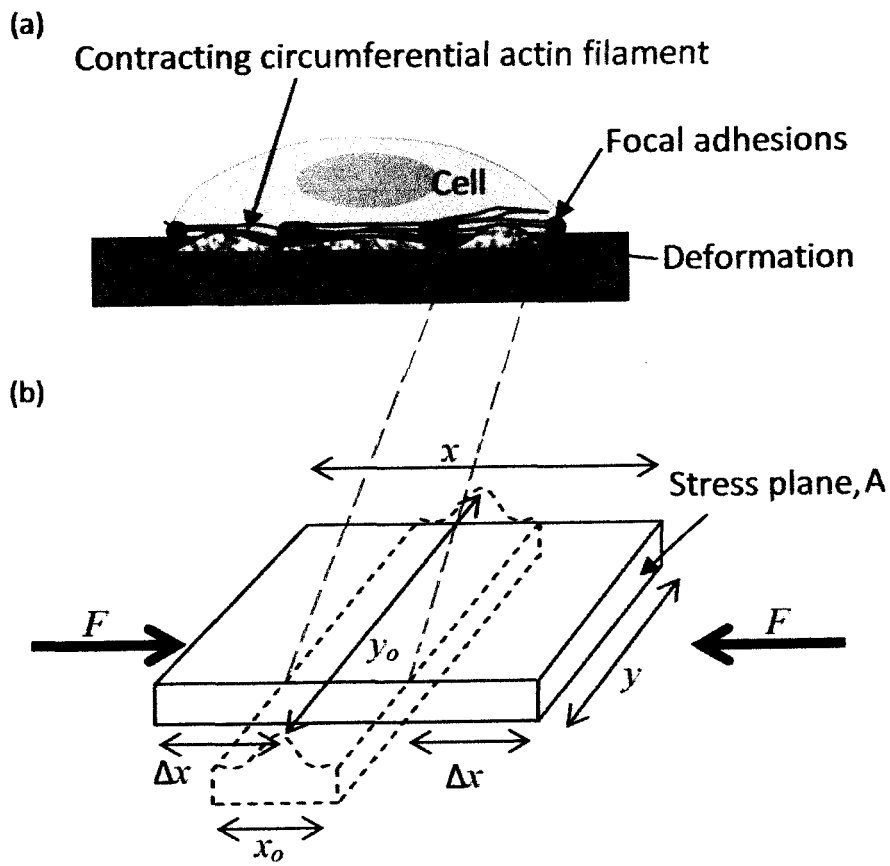


Figure 2-1. (a) Schematic diagrams showing lateral view of a cell inducing deformations in the liquid crystal surface due to the contractions of circumferential actin filaments exerting traction forces via focal adhesions. (b) A constitutive model showing the dimensions of a stress site in LC surface before (solid line) and after (broken line) the compressive force (F) applied to the stress plane (A). (x, y) and (x_0, y_0) are the dimensions of biaxial deformation during relaxation and contraction, respectively. The parameters, x and y , are the dimensions in transverse and longitudinal directions, respectively.

For each of the phase contrast micrographs containing a cell before and after treatment with cytochalasin-B for a period of 30 minutes, the strain profiles of a deformation line (x, y, x_0 and y_0) in the LC surface were determined as defined in Figure 2-1. The dimensions, x_0 and y_0 are the width and length of a deformation line before cytochalasin-B treatment, while, x and y are the same parameters after

cytochalasin-B treatment. The length of the contact area was assumed to be equivalent to y (Figure 2-1). When a cell is exerting forces on a substrate at the focal adhesions, it is estimated that a maximum of three cylindrical shaped focal adhesion molecules of regular size can be recruited [37, 38]. The occurrence of the focal adhesion at regular width was as observed in Peterson et al. 2004. These uniform focal adhesions become stabilized in stationary keratinocytes (Mohl et al 2009, Peterson et al. 2004). Therefore, the height, h , of the cylindrical focal adhesions was estimated by three times the diameter ($3 \times d$) of a stained vinculin. Increased stresses within a cell are transmitted from the actin cytoskeleton to the substrate via these stabilized focal adhesions. The applied forces are then dependent on the variation in the length and width of the LC deformation lines formed. The diameter of a stained vinculin can be measured from the immuno-stained micrographs of the vinculins. The transverse displacement (Δx) was obtained by taking half of the difference between the width of deformation lines before and after cell treatment with cytochalasin-B, where $\Delta x = (x - x_0)/2$ (Figure 2-1).

Having determined the strains in relation to the cell induced deformation lines in the LC together with the Young's modulus of the LC, the traction forces applied to the stress planes (A) of the liquid crystals were estimated by using Hooke's equation as, $F = (EA\Delta x)/x$, where E is the Young's modulus, A is the assumed focal contact area or $(y \times h) \mu\text{m}^2$, Δx is the transverse displacement and x is the original length of the stress site in the LC surface as shown in Figure 2-1.

2.2.6 Development of a cell traction force measurement and mapping software

The bespoke CTFM software incorporated with a graphical user interface (GUI) was developed using the MATLAB Integrated Development Environment (IDE). The software functions to map localized cell traction forces based on the CTF-longitudinal deformation relationship of the liquid crystals as quantified from the cell relaxation experiments.

The CTFM software was developed to be as user friendly as possible in order to generate a cell traction force map for further analysis. The full details of the design and execution of the program are as illustrated in Supplement A.

2.3 Results and discussion

The Young's moduli of the liquid crystals determined by using spherical indentation technique were similar and highly reproducible. The result of the spherical indentation and discussion are available in Appendix A. The mean and standard deviation (mean \pm SD) of the Young's modulus for the three independent samples of liquid crystals are 89.5 ± 15.5 kPa, 87.3 ± 18.5 kPa and 84.7 ± 17.7 kPa, respectively. For the cholesteryl ester liquid crystals, the total average of the Young's modulus for the three repeats of experiment was 87.1 ± 17.2 kPa. This range of Young's modulus is comparable to the Young's modulus (108 ± 20 kPa) of the LC determined using AFM nano-indentation technique as reported in [39]. The experimental work reported by [40] shows via AFM that the Young's modulus of the normal human keratinocyte cytoskeleton ranges from 120 – 340 kPa (mean \pm SD = 182 ± 58 kPa). In addition, the Young's modulus of skin was reported at 129 ± 88 kPa (mean \pm SD) and 82 ± 60 kPa (mean \pm SD) by using suction method [41, 42], respectively. Therefore, the Young's modulus of the LC surface seems to be in good agreement to the stiffness of the keratinocytes and human skin. This is an added advantage of our cell force transducer because the elastic modulus of the liquid crystals may provide suitable mechanical signals that are similar to those of the in-vivo environment (skin) whilst being able to support cell adhesion [43, 44].

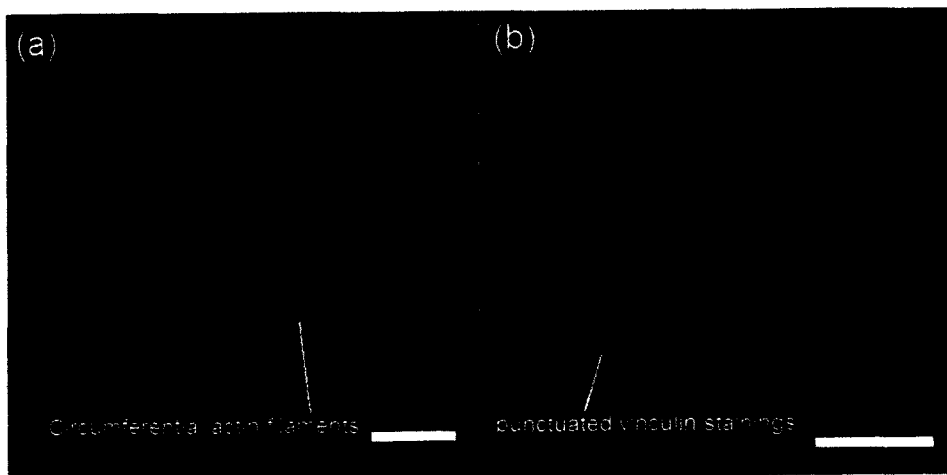


Figure 2-2. Fluorescence micrographs of staining against (a) actin filaments, and (b) vinculin for keratinocytes cultured on the liquid crystal substrates.

(Scale bar: 25 μ m)

The results of the fluorescence staining experiments indicated that keratinocytes cultured on the LC substrates contained short circumferential actin filaments at the periphery (Figure 2-2a). The cells in similar cultures were also stained positively for punctuated vinculin accumulations which were mostly distributed at the margin of the cells (Figure 2-2b). These results were reproducible. These stained vinculin accumulations have a length and diameter of approximately $1.05 \pm 0.04 \mu\text{m}$ and $0.26 \pm 0.01 \mu\text{m}$ (mean \pm SE), respectively. The size of vinculins determined in this work is lower than the typical length of 'classical' focal adhesions (2 - 6 μm) [37] which is probably associated with the stiffness of the liquid crystals. When culturing cells on a soft substrate, the mechanical signal from the extracellular matrix induces disassembly of the focal adhesion proteins via the Rho-GTPase pathways, which in turn promotes de-phosphorylation of the actin cytoskeleton driven by Myosin II [45]. The results suggest that the arrangements of the actin filaments and focal adhesions influence the characteristics of cell attachments, and thus affect the distribution of CTFs on the soft surface of liquid crystals.

Prior to the cell relaxation experiment, HaCaTs were found to attach to the LC substrates after 24 hours of incubation. These cells were found to induce traction forces causing the formation of short LC deformation lines at the boundary of the cells [20]. Based on the ten phase contrast micrographs of cells adhering to the LC surface, each of the ten cells studied induced an average of 4 - 6 deformation lines in the LC surface. For example, in Figure 2-3a, a rounded quiescent keratinocyte was observed; the cell induced short radiating LC deformation lines from its periphery. An example of a LC deformation line induced by this cell (marked by measurement lines in Figure 2-3a) had a width (x_0) and length (y_0) of $2.02 \mu\text{m}$ and $4.64 \mu\text{m}$, respectively. After treating the cell with cytochalasin-B for 30 minutes, the forces applied by the cell tangentially on the LC surface were released in opposite directions (Figure 2-3b). As a result, the width (x) and length (y) of that deformation line resized to $4.57 \mu\text{m}$ and $1.72 \mu\text{m}$, respectively. After treatment with cytochalasin-B for 60 minutes, the cell took on a more flattened morphology and the LC deformation lines disappeared entirely (Figure 2-3c). In order to obtain accurate measurement of the displacements, only those individual deformation lines that are not clustered with other deformation lines were used for quantification in the repeat of experiments. One of the examples is as marked in Figure 2-3a. This LC

deformation was induced by a pair of cell traction forces at ~ 82 nN that were determined using Hooke's equation. The spatial resolution of the well-defined and isolated deformation lines was approximately $\sim 1 - 2$ μm (Figure 2-3d).

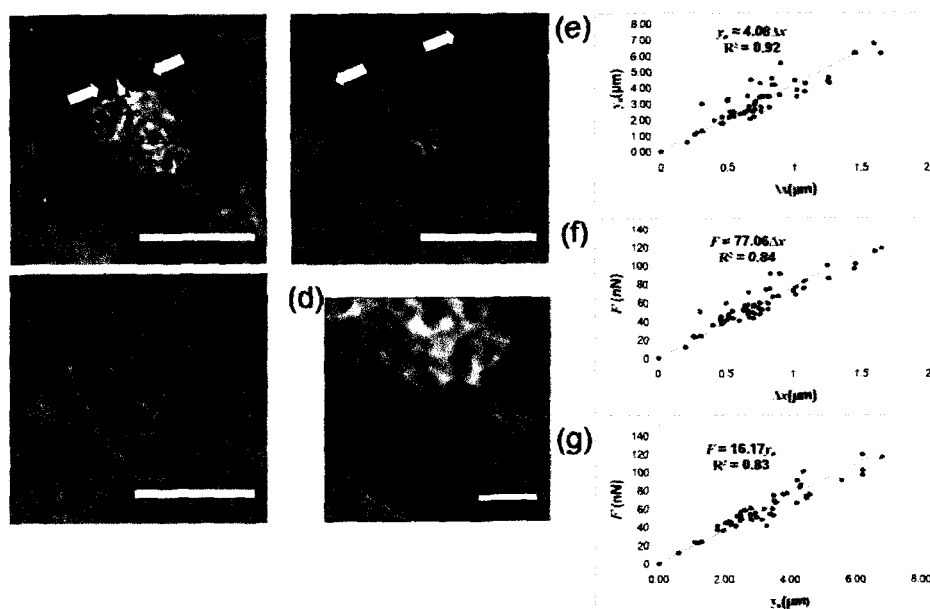


Figure 2-3. Phase contrast images of a cell treated with 30 μM cytochalasin-B at (a) 0 minute, (b) 30 minute and (c) 60 minutes on the surface of the liquid crystals (Scale bar: 20 μm); (d) Enlarged exert of a box in (a) showing the width of the deformation lines formed in the LC surface, (Scale bar: 10 μm). The inward and outward arrows show the directions of the applied and released forces at a stress site, respectively. (e) Transverse displacement (Δx) versus the length of longitudinal deformation (y_0), (f) cell traction force (F) versus the transverse displacement (Δx), and (g) cell traction force (F) versus the length of longitudinal deformation (y_0) for 55 deformation lines.

Clearly, the results indicate that the pair of compressive stresses applied transversely at the stress site (represent by inward arrows in Figure 2-3a) induced shear forces in x and y directions resulting in a deformation line as depicted in the model of Figure 2-1. The orientation of the LC deformation lines can be in arbitrary directions, depending on the location of the CTFs that are applied in perpendicular to the deformation lines [20]. Each linear deformation formed at a local region of LC surface was in good agreement with the biaxial deformation associated with the

Poisson's ratio or small deformation theory [46]. The strain in z plane was indicated by phase differences in the phase contrast images but this was difficult to measure via microscopy.

From the cell relaxation and fluorescence staining experiments, the results indicate that the transverse shear forces induced in x direction most likely originate from the contraction of short circumferential actin filaments involved in maintaining the morphology of keratinocytes. This regulation of cell shape is adhesion dependent [47, 48], and therefore remodeling of the actin cytoskeleton system requires the exertion of CTFs to a surface.

The procedures used in determining the CTF were repeated for ten single cells, in which, 55 deformation lines were analyzed. In the quantification of CTF, the relationships among the transverse displacement (Δx), length of longitudinal deformation (y_o) of the liquid crystals and the cell traction force (F) were derived (Figure 2-3e-g). Figure 2-3e shows that $y_o \leq 8 \mu\text{m}$ (thickness of LC substrate = $100 \mu\text{m}$) which is well within the linear viscoelastic range ($< 10\%$ shear strain) of the liquid crystals [19]. By referring to the Poisson's equation, $\nu = [(y-y_o)/y_o]/[(x_o-x)/x_o]$, (Tschoegl et al., 2002), the ratio of y_o to Δx at about 4 is the determinant for the Poisson's ratio to be around 0.5. Therefore, the linear relationship of y_o to Δx by a coefficient of 4.08 (Figure 2-3e) provides a strong indication that the liquid crystals have a Poisson's ratio of approximately 0.5. The transverse displacement (Δx in μm) and length of longitudinal deformation (y_o in μm) induced in the LC surface increased linearly with the CTF exerted at a factor of $77.06 \text{ nN}/\mu\text{m}$ and $16.17 \text{ nN}/\mu\text{m}$, respectively (Figure 2-3f-g). By using the least square method, the standard error of the linear regression line, $F = 16.17y_o$, was determined at $0.34 \text{ nN}/\mu\text{m}$. The 95% confidence interval for the coefficient of this slope was $15.49 < \text{mean of the slope} < 16.83 \text{ nN}/\mu\text{m}$. The traction forces of keratinocytes measured per LC deformation were found to range between $10 - 120 \text{ nN}$ (Figure 2-3f-g) and the mean CTF was $58 \pm 3 \text{ nN}$ (mean \pm SE). However, the overall measurements of every traction force are accounted to the variability of the Young's modulus of the liquid crystals and the estimated height of the focal adhesions and therefore, the propagation of error due to these two factors were derived and calculated at 23% (Appendix A) [49, 50]. Such variability is reasonable for a measurement involving a semi-solid material and biological entity. The relationship between CTF and

longitudinal deformation (F versus y_o) established in this study can be used to rapidly estimate the traction forces induced by a cell if the length of the deformation line is known. Thus, this relationship was used to compute the traction forces of cells in our custom-built CTFM software.

In the CTFM software, the length of the deformation lines measured were automatically converted into CTFs by using the linear CTF-longitudinal deformation coefficient (16.17 nN/ μ m). Figure 2-4a shows the magnitude and location of each CTF assigned in the Euclidean coordinate system. The data points of the CTF were then rendered into a 3D force distribution map as shown in Figure 2-4b. The intensity of the force in nano-Newton (nN) was represented by pseudo colors in a scale bar. The result showed that the spatial resolution of this CTFM software is approximately 3 μ m [51]. A detail explanation of the interactive GUI used in the measurements of the CTF is beyond the scope of this paper.

Figure 2-4c and Figure 2-4d show other examples of single HaCaT cells inducing deformation lines in the surface of liquid crystals after culturing at 37 °C for 24 hours. As shown in Figure 2-4a and Figure 2-4c, the morphology of single non-polarized keratinocytes on the liquid crystals is generally polygonal or rounded which is consistent with the observations reported in [52, 53]. For these two non-polarized cells, the detected CTFs were indicated by isolated deformation lines (y_o) of various lengths (0.6 – 4.6 μ m) in the LC surface. Discrete and isolated forces of between 10 and 80 nN were found distributing evenly at the boundary of these quiescent cells (Figure 2-4b and c, right). For these cells, the peak forces indicated as red regions in the figures were observed as 65 nN and 80 nN, respectively. In contrast, an elongated cell or polarized cell (Figure 2-4d) induced higher traction forces at one end of the cell (Figure 2-4d, right). Consistent with the report in [52], polarized keratinocytes on the LC surface are characterized by elongated morphology with lamellipodia distributed at the terminals of the cell. The result shows that the peak force determined for a polarized keratinocyte (~180 nN) is greater than those of the non-polarized keratinocytes (~ 60 - 80 nN). This result also indicates that the traction forces expressed by cells on the LC surface are highly associated with the restructuring of actin cytoskeleton and the morphology changes of a cell. Our LCTFT system has demonstrated high sensitivity to detect and distinguish various CTF magnitudes and morphological changes in cells. This

sensing ability is one of the fundamental requirements of a CTF sensor for use in the study of cell migration.

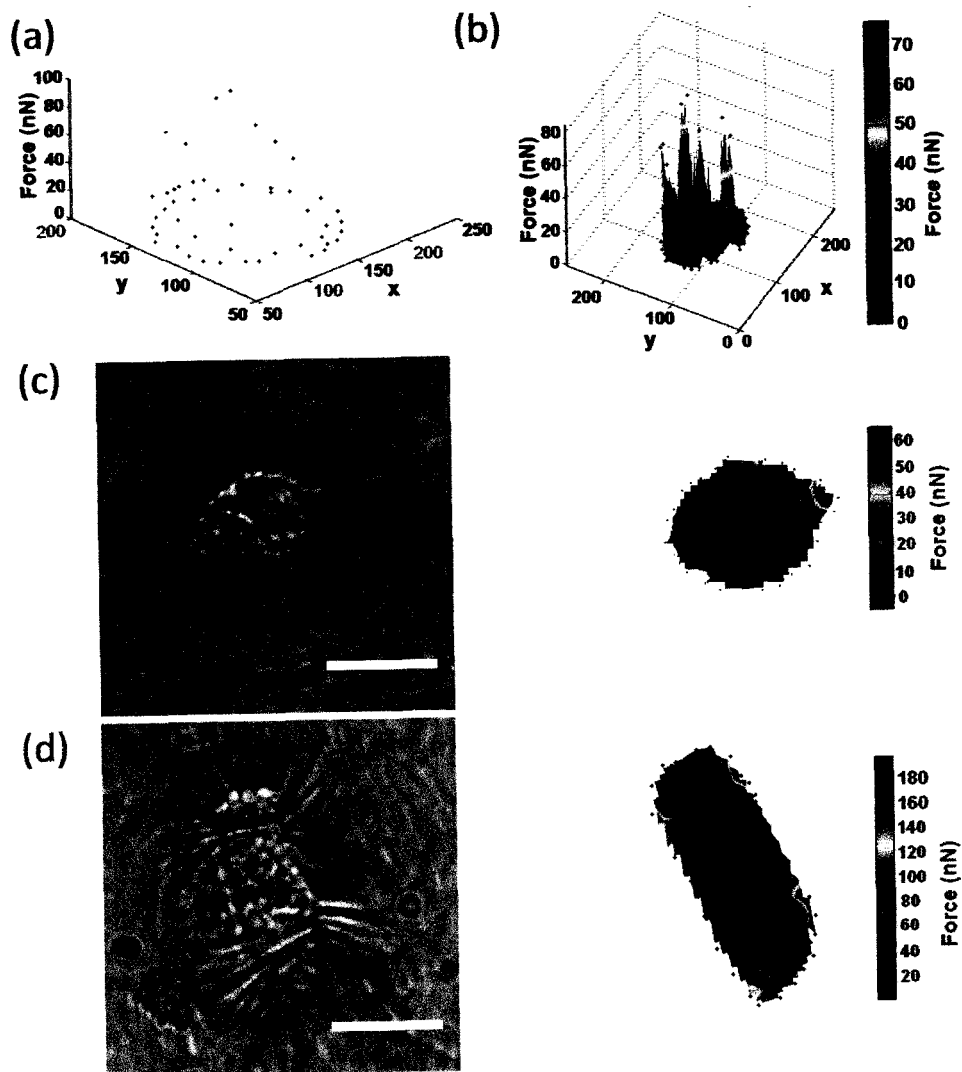


Figure 2-4. (a) Distribution of cell traction force points on a Euclidean coordinate system and (b) the associated 3D force map rendered in pseudo-colors. Phase contrast photomicrographs of (c) a single quiescent and (d) a polarized HaCaTs contracting on the LC based CTF transducer. Images on the right of (c) and (d) are the associated force maps for the cells in (c) and (d), respectively. The scale bar in pseudo colors represents the intensity of the cell traction forces in nano-Newton. (Scale bar: 20 μm)

Studies on keratinocyte derived traction forces are very limited. A recent study used bead-labeled PDMS substrate technique to probe traction forces of keratinocytes [54]. It was reported that the traction forces found for individual focal adhesion of migrating keratinocytes were approximately 8.6 ± 0.54 nN (mean \pm SE). In comparison, our work measured marginally higher traction forces (58 ± 22 nN, mean \pm SD) for keratinocytes exerted at a localized stress region with a 95% confidence of ± 6.2 nN. This could be due to the nature of the liquid crystal surface which is characterized by a flexible continuum allowing CTFs to be transmitted via clusters of focal adhesion at local regions. However, the range of CTFs determined in our study (10 – 120 nN) approximates CTFs measured using the micro-patterned PDMS ranging between 5 - 35 nN for Madin-Darby canine kidney (MDCK) epithelial cells [55]. In addition, our results seem to agree with the traction forces of epithelial cells measured using other techniques [56, 57]. Sagvolden and co-worker show that the cervical carcinoma cell required 100 - 200 nN to dissociate from an AFM cantilever [56]. Similarly, a report by Thoumine et al. shows that an epithelial cell line (HBL100) required an exposure of 100 nN tangential force to detach from a surface in a centrifugation system [57].

The sensitivity of the LC based CTF transducer to a wide range of CTFs may be associated with cholesteryl chloride in the mixtures of cholesteryl ester liquid crystals which provides the shear sensitivity of the liquid crystals [28]. The precision of the liquid crystal transducer can be further improved by studying the in-situ expression of vinculin which obtained the exact contact depth of the focal adhesion in the calculation of the cell traction force. The localized responses of the LCTFT to the CTF at a minimum spatial resolution of approximately 1 μ m could be due to the discrete arrangement of the liquid crystal molecules. When the applied CTFs overcome the cohesion forces of the LC molecules, the LC molecules tilt or deflect accordingly to the intensity of the applied CTFs via the focal adhesions. The forces were transmitted in a finite confined region and the shear energy induced does not propagate to the surrounding mesogens. This allows the LCTFT to detect CTF at high spatial resolutions (see Figure 2-3d). The LCTFT technique also allows dispersion of contacts in arbitrary directions on a two-dimensional continuum. Unlike the fluorescence marker displacement techniques, our technique does not require a null-force reference image to track the randomly dispersed markers, and hence enables direct inference of cell traction in real time [6, 7]. While having the

same capabilities [20, 58], LCTFT has advanced the wrinkle-based technique by demonstrating a higher sensitivity and linear viscoelasticity along with an improved spatial resolution in detecting localized traction forces of cells. TGF-beta 1 is a cytokine used in wound healing that has been shown to induce stress fibers response in fibroblasts via immunofluorescence imaging. By using traditional organ bath based method to test the effects of this cytokine on a section of tissue, the response of a single cell type cannot be determined. However, via single cell-LC based force transducer system, we demonstrated that the transducer is very sensitive and able to measure changes in contraction forces in response to different doses of TGF-beta 1 [59]. It is expected that the new LCTFT incorporating the CTFM software system will have applications for measuring traction forces in a range of different cell types and potentially generating a new single cell-LC based pharmacological assays in the context of wound healing.

CHAPTER 3

INTERFACIAL STUDY OF CELL ADHESION TO LIQUID CRYSTALS USING WIDEFIELD SURFACE PLASMON RESONANCE MICROSCOPY

3.1 Introduction

A challenge to cell based biosensor development is being able to achieve effective sensing of cell responses within support media which are chemically and rheologically compatible. To this end, our previous work has examined the emerging application of liquid crystal thin films in single cell force sensing using conventional optical microscopy [5]. These liquid crystal based biosensors enable cell adhesion and contractile activity to change the organization of the liquid crystals leading to the detection of cell responses [19, 22, 60-62]. Our study [62] indicated that cholesteryl ester liquid crystals can support cell adhesion and allow the *detection of cellular contractions without pre-coating the liquid crystals with adhesion ligands*. Although cell-surface interactions have recently been examined with liquid crystals functioning as the force transducer, it is not understood how soft substrates such as liquid crystals affect the organization of the focal adhesions that *enable cell attachment to a culture substrate*.

Surface plasmons (SP) are highly sensitive to dielectric permittivity changes on a metal-dielectric surface [63]. Thus, surface plasmon technology has been used in the development of light microscope system in which differences in the optical densities of the imaging target alter the way p-polarized light couples into surface plasmons. This results in varying amount of light reflected from a metallic coated surface such as a gold coated glass substrate [64]. This means that surface plasmon microscopy allows the acquisition of a sample image in which contrast is dependent

REFERENCE

- [1] T. Oliver, *et al.*, "Design and use of substrata to measure traction forces exerted by cultured cells," *Methods in Enzymology*, vol. 298, pp. 497-521, 1998.
- [2] K. Burton and D. L. Taylor, "Traction forces of cytokinesis measured with optically modified substrata," *Nature*, vol. 385, pp. 450-454, 1997.
- [3] Y. Xia and M. Karin, "The control of cell motility and epithelial morphogenesis by Jun kinases.," *Trends in Cell Biology*, vol. 14, pp. 94-101, 2004.
- [4] K. Beningo, *et al.*, "Flexible polyacrylamide substrata for the analysis of mechanical interactions at cell-substratum adhesions.," *Methods in Cell Biology*, vol. 69, pp. 325-339, 2002.
- [5] K. A. Beningo, "Flexible substrata for the detection of cellular traction forces," *Trends in Cell Biology*, vol. 12, pp. 79-84, 2002.
- [6] T. Oliver, *et al.*, "Traction forces in locomoting cells," *Cell Motility and the Cytoskeleton* vol. 31, pp. 225-240, 1995.
- [7] M. Dembo and Y.-L. Wang, "Stresses at the cell-to-substrate interface during locomotion of fibroblasts," *Biophysical Journal*, vol. 76, pp. 2307-2316, 1999.
- [8] K. Burton, *et al.*, "Keratocytes generate traction forces in two phases," *Molecular Biology of the Cell*, vol. 10, pp. 3745-3769, November 1999.
- [9] M. T. Ghannam and M. N. Esmail, "Rheological Properties of Poly(dimethylsiloxane)," *Indian Engineering Chemistry Research* vol. 37, pp. 1335-1340, 1998.
- [10] M. T. Ghannam and M. N. Esmail, "Rheological properties of aqueous polyacrylamide solutions," *Journal of Applied Polymer Science*, vol. 69, pp. 1587-1597, 1998.
- [11] G. Hinrichsen, *et al.*, "Mechanical behaviour of cerclage material consisting of silicon rubber," *Graefes Archiv Ophthalmologie*, vol. 211, pp. 251-258, 1979.
- [12] K. Addae-Mensah and J. Wikswo, "Measurement techniques for cellular biomechanics in vitro," *Experimental Biology and Medicine (Maywood)*, vol. 233, pp. 792-809, 2008.
- [13] J. H.-C. Wang and J.-S. Lin, "Cell traction force and measurement methods," *Biomechanics and Modeling in Mechanobiology*, vol. 6, pp. 361-371, 2007.
- [14] A. Pathak, *et al.*, "The simulation of stress fibre and focal adhesion development in cells on patterned substrates," *Journal of Royal Society Interface*, vol. 5, pp. 507-524, 2008.
- [15] S. Britland, *et al.*, "Morphogenetic guidance cues can interact synergistically and hierarchically in steering nerve cell growth," *Experimental Biology Online*, vol. 1, pp. 1-15, 1996.